



Effects of alternating and direct current in electrocoagulation process on the removal of cadmium from water

Subramanyan Vasudevan*, Jothinathan Lakshmi, Ganapathy Sozhan

CSIR-Central Electrochemical Research Institute, Karaikudi 630 006, India

ARTICLE INFO

Article history:

Received 7 February 2011

Received in revised form 15 April 2011

Accepted 18 April 2011

Available online 14 May 2011

Keywords:

Electrocoagulation

Alternating/direct current

Cadmium removal

Adsorption kinetics

Isotherms

ABSTRACT

In practice, direct current (DC) is used in an electrocoagulation processes. In this case, an impermeable oxide layer may form on the cathode as well as corrosion formation on the anode due to oxidation. This prevents the effective current transfer between the anode and cathode, so the efficiency of electrocoagulation processes declines. These disadvantages of DC have been diminished by adopting alternating current (AC) in electrocoagulation processes. The main objective of this study is to investigate the effects of AC and DC on the removal of cadmium from water using aluminum alloy as anode and cathode. The results showed that the removal efficiency of 97.5 and 96.2% with the energy consumption of 0.454 and 1.002 kWh kl⁻¹ was achieved at a current density of 0.2 A/dm² and pH of 7.0 using aluminum alloy as electrodes using AC and DC, respectively. For both AC and DC, the adsorption of cadmium was preferably fitting Langmuir adsorption isotherm, the adsorption process follows second order kinetics and the temperature studies showed that adsorption was exothermic and spontaneous in nature.

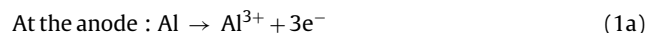
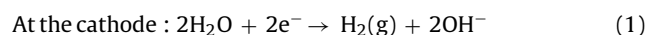
© 2011 Elsevier B.V. All rights reserved.

1. Introduction

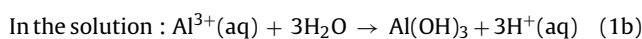
Heavy metal pollution has become one of the most serious environmental problems today. The treatment of heavy metals is of special concern due to their recalcitrance and persistence in the environment. Unlike organic contaminants, heavy metals are not biodegradable and tend to accumulate in living organisms and many heavy metal ions are known to be toxic or carcinogenic. Toxic heavy metals of particular concern in treatment of industrial wastewaters include zinc, copper, nickel, mercury, cadmium, lead and chromium. Cadmium is one of the most toxic non-essential heavy metals present in the environment, even at low concentrations. Elevated level of cadmium ions arise from a variety of sources such as wastewater from metal plating industries, nickel–cadmium batteries, phosphate fertilizer, mining, pigments, stabilizers, alloys, petroleum refining, welding and pulp industries [1–3]. Cadmium poisoning includes kidney damage [4], lung insufficiency, cancer; it changes the constitution of bone, liver and blood [5]. Cadmium accumulated in the rice crops, it developed Itai-Itai disease and renal abnormalities including proteinuria and glucosuria. Cadmium containing compounds are known as carcinogens [6,7]. The drinking water guideline value is 0.005 mg/L [8].

Conventional methods for removing cadmium from water include ion exchange, reverse osmosis, co-precipitation, coagulation, complexation, solvent extraction, electrochemical treatment and adsorption [9–25]. Physical methods like ion exchange, reverse osmosis and electro dialysis have proven to be either too expensive or inefficient to remove cadmium from water. At present, chemical treatments are not used due to disadvantages like high costs of maintenance, problems of sludge handling and its disposal, and neutralization of the effluent [26]. The cadmium removal from water by adsorption using different materials has also been explored. The major disadvantages of this studied adsorbent are low efficiency and high cost. Recent research has demonstrated that electrocoagulation offers an attractive alternative to above-mentioned traditional methods for treating water [27]. In this process anodic dissolution of metal electrode takes place with the evolution of hydrogen gas at the cathode [28]. Electrochemically generated metallic ions from the anode can undergo hydrolysis to produce a series of activated intermediates that are able to destabilize the finely dispersed particles present in the water to be treated. The destabilized particles then aggregate to form flocks as outlined below,

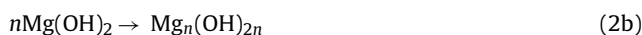
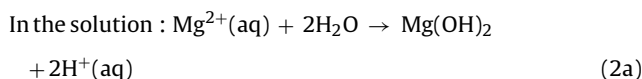
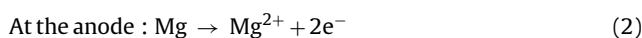
- (i) When aluminum is used as electrode, the reactions are as follows:



* Corresponding author. Tel.: +91 4565 227554; fax: +91 4565 227779.
E-mail addresses: vasudevan65@gmail.com, svdevan.2000@yahoo.com (S. Vasudevan).



(ii) When magnesium is used as the electrode, the reactions are as follows:



The advantages of electrocoagulation include high particulate removal efficiency, a compact treatment facility, relatively low cost, and the possibility of complete automation. This method is characterized by reduced sludge production, a minimum requirement of chemicals and ease of operation [29–31].

In general, direct current (DC) is used in an electrocoagulation processes. In this case, an impermeable oxide layer may form on the cathode as well as corrosion formation on the anode due to oxidation. These prevent the effective current transport between the anode and cathode, so the efficiency of electrocoagulation processes declines. These disadvantages of DC have been overcome by adopting alternating current (AC) in electrocoagulation processes. The main objective of this study is to investigate the effect of AC on the removal efficiency of cadmium using aluminum alloy as anode and cathode. The effect of the initial concentration of cadmium ion, pH, temperature, current density and coexisting ions were investigated. The adsorption kinetics of cadmium ions on aluminum hydroxide is also studied. For this, equilibrium adsorption behaviour is analyzed by fitting the Langmuir and Freundlich isotherm models. The adsorption kinetics of electrocoagulation was analyzed using first, second order kinetic models. Finally, the effects of temperature were studied to determine the nature of adsorption.

2. Materials and methods

2.1. Cell construction and electrolysis

Fig. 1 shows the electrolytic cell consisting of a 1.0-L Plexiglas vessel that was fitted with a polycarbonate cell cover with slots to introduce the anode, cathode, pH sensor, a thermometer and electrolytes. Aluminum alloy consisting of Zn (1–4%), In (0.006–0.025%), Fe (0.15%), Si (0–.15%) (CSIR-CECRI, India), with a surface area of 0.2 dm² acted as the anode and cathode, respectively and placed at an interelectrode distance of 0.005 m. The temperature of the electrolyte has been controlled to the desired value with a variation of ± 2 K by adjusting the rate of flow of thermostatically controlled water through an external glass-cooling spiral. A regulated direct current (DC) was supplied from a rectifier (10 A, 0–25 V; Aplab model) and regulated alternating current (AC) was supplied from a source (0–5 A, 0–270 V, 50 Hz; AMETEK Model: EC100S).

Cadmium nitrate Cd(NO₃)₂·4H₂O (Analar Reagent) was dissolved in tap (drinking) water for the required concentration. In all the experiments 20 mg/L of cadmium was used. The pH of the electrolyte was adjusted, if required, with HCl (1 mol/L) or NaOH (1 mol/L) solutions before adsorption experiments. To study the effect of co-existing ions, in the removal of cadmium, sodium salts (Analar Grade, Merck, Germany) of phosphate (0–50 mg/L), silicate (0–15 mg/L), carbonate (0–250 mg/L) and arsenic (0–5.0 mg/L) was added to the electrolyte.

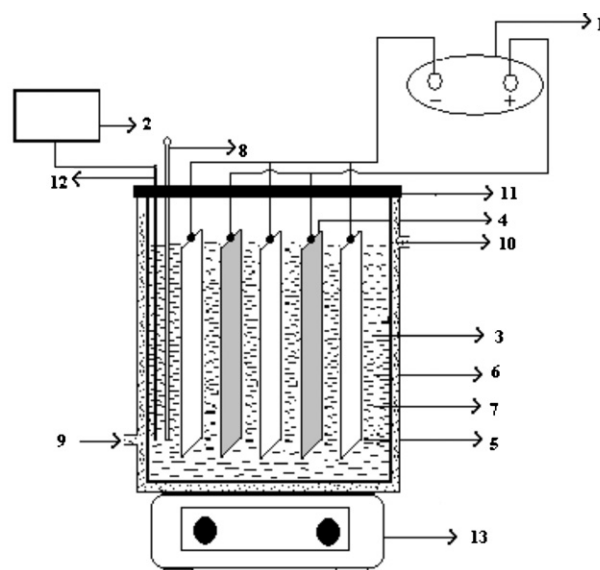


Fig. 1. Laboratory scale cell assembly. (1) DC power supply; (2) pH meter; (3) electrochemical cell; (4) cathodes; (5) anode; (6) electrolyte; (7) outer jacket; (8) thermostat; (9) inlet for thermostatic water; (10) outlet for thermostatic water; (11) PVC cover; (12) pH sensor and (13) magnetic stirrer.

2.2. Analytical method

The concentration of cadmium was determined using UV-visible Spectrophotometer with cadmium kits (MERCK, Pharo 300, Germany). The SEM and EDAX of cadmium adsorbed aluminum hydroxide coagulant were analyzed with a Scanning Electron Microscope (SEM) made by Hitachi (model s-3000 h). The Fourier transform infrared spectrum of aluminum hydroxide was obtained using Nexus 670 FTIR spectrometer made by Thermo Electron Corporation, USA. The XRD for aluminum hydroxide coagulant was analyzed by X-ray diffractometer made by JEOL X-ray diffractometer (type – JEOL, Japan). The concentration of carbonate, silicate, arsenic and phosphate were determined using UV-Visible Spectrophotometer (MERCK, Pharo 300).

3. Results and discussion

3.1. Effect of current density

The amount of cadmium removal depends upon the quantity of adsorbent (aluminum hydroxide) generated, which is related to the time and current density. The amount of adsorbent [Al(OH)₃] was determined from the Faraday law

$$E_c = \frac{ItM}{ZF} \quad (3)$$

where I is the current in (A), t is the time (s), M is the molecular weight, Z is the electron involved, and F is the faraday constant (96485.3 C/mol). To investigate the effect of current density on the cadmium removal, a series of experiments were carried out by solutions containing constant cadmium loading of 20 mg/L, at a pH 7.0, with current density being varied from 0.1 to 0.5 A/dm² using both AC and DC current source. The results are presented in Table 1. The results show that the removal efficiency of cadmium was higher and energy consumption was lower in the case of AC than DC. This may be due to the uniform dissolution of anode and cathode during electrocoagulation in the case of AC. The removal efficiency was found showing the amount of cadmium adsorption increases with the increase in adsorbent concentration, which indicates that

Table 1
Effect of current density on the removal efficiency of cadmium using AC and DC with initial cadmium concentration 20 mg/L.

Current density (A/dm ²)	AC		DC	
	Removal efficiency (%)	Energy consumption (kWh kl ⁻¹)	Removal efficiency (%)	Energy consumption (kWh kl ⁻¹)
0.1	94.0	0.227	92.4	0.881
0.2	97.5	0.454	96.2	1.002
0.3	97.9	0.574	97.1	1.214
0.4	98.5	0.581	97.5	1.336
0.5	99.0	0.639	97.9	1.458

the adsorption depends up on the availability of binding sites for cadmium.

3.2. Effect of pH

The adsorption behaviour of cadmium has been investigated at different pH values ranging from 4.0 to 9.0 using AC and DC source. The percentage of cadmium adsorption increased with increasing pH 7, a decreasing trend in adsorption was observed when below and above pH 7 for both AC and DC source. At an initial concentration of 20 mg/L, maximum adsorption of 97.5% and 96.2% at pH 7 for AC and DC source (Fig. 2). According to the literature pH of precipitation of cadmium starts at pH 8.2 [32], so in higher pH removal efficiency was low. At low pH, Cd²⁺ ions had to compete with H⁺ ions for adsorption sites on the adsorbent surface. As the pH increased, this competition weakens and more Cd⁺ ions were able to replace H⁺ ions bound to the adsorbent surface.

3.3. Effect of initial cadmium concentration

To study the effect of initial concentration, experiments were conducted at varying initial concentrations from 10 to 50 mg/L using AC and DC. The removal of Cd(II) increased with time to obtain equilibrium at about 30 min (Fig. 3). The amount of cadmium adsorbed (q_e) increased from 6.42 to 49.61 mg/g as the concentration was increased from 10 to 50 mg/L for the AC source. The figure also shows that the adsorption is the rapid in the initial stages and gradually decreases with progress of adsorption this is because of the great number of sites available for the sorption operation and adsorption equilibrium were then gradually achieved. The plots are single, smooth and continuous curves leading to saturation, suggesting the possible monolayer coverage to cadmium on the surface

of the adsorbent [33]. In the case of DC the equilibrium time was found to be 45 min for all concentration studied (figure not shown).

3.4. Adsorption kinetics

The kinetics of removal of cadmium is explicitly explained in the literature using first-order and second-order kinetic models. The adsorption of cadmium is analyzed using Lagergran rate equation. The first order Lagergran model is [34,35].

$$\frac{dq}{dt} = k_1(q_e - q_t) \quad (4)$$

where, q_t is the amount of cadmium adsorbed on the adsorbent at time t (min) and k_1 (1/min) is the rate constant of first order adsorption. The integrated form of the above equation with the boundary conditions $t=0$ to >0 ($q=0$ to >0) and then rearranged to obtain the following time dependence function,

$$\log(q_e - q_t) = \log(q_e) - \frac{k_1 t}{2.303} \quad (5)$$

where q_e is the amount of cadmium adsorbed at equilibrium. The q_e and rate constant (k_1) were calculated from the slope of the plots of $\log(q_e - q_t)$ versus time (t) (figure not shown). It was found that the calculated q_e value do not agrees with the experimental q_e values.

The second order kinetic model is expressed as [36]

$$\frac{dq}{dt} = k_2(q_e - q_t)^2 \quad (6)$$

where k_2 is the rate constant of second order adsorption. The integrated form of Eq. (6) with the boundary condition $t=0$ to >0 ($q=0$ to >0) is

$$\frac{1}{(q_e - q_t)} = \frac{1}{q_e} + k_2 t \quad (7)$$

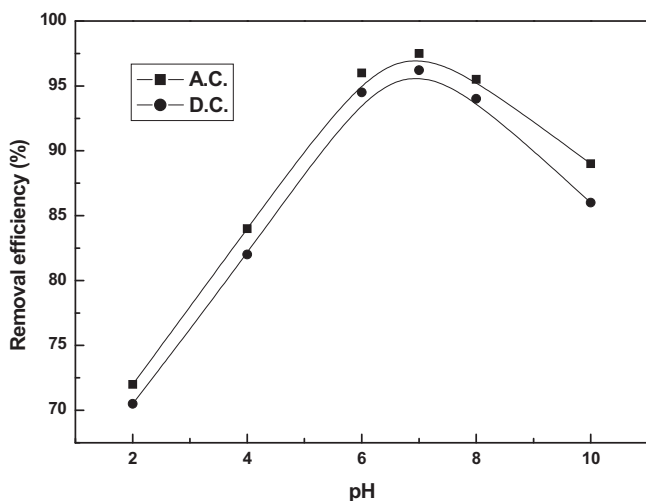


Fig. 2. Effect of pH of the electrolyte on the removal of cadmium. Conditions: electrolyte concentration of 20 mg/L; current density of 0.2 A/dm²; temperature of 303 K.

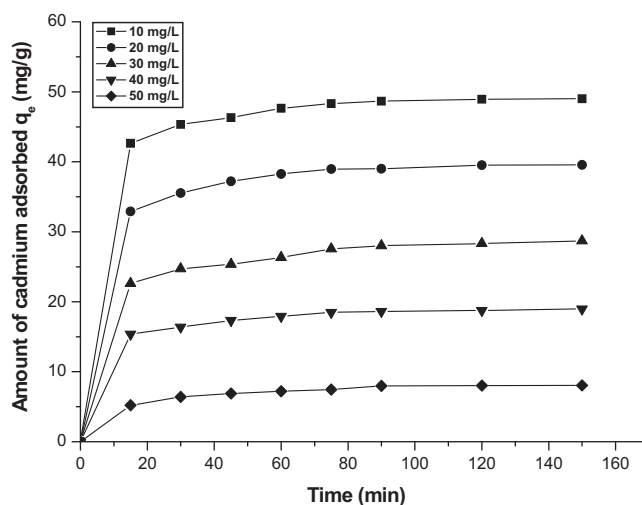


Fig. 3. Effect of electrolysis time and amount of cadmium adsorbed for AC. Conditions: current density of 0.2 A/dm²; pH of 7.0; temperature of 303 K.

Table 2

Comparison between the experimental and calculated q_e values for different initial cadmium concentrations in first and second order adsorption isotherm at temperature 305 K and pH 7.

Current source	Concentration (mg/L)	q_e (exp)	First order adsorption			Second order adsorption		
			q_e (Cal)	$K_1 \times 10^3$ (min/mg)	R^2	q_e (Cal)	$K_2 \times 10^3$ (min/mg)	R^2
AC	10	6.42	46.32	-0.0033	0.7851	7.01	2.221	0.9999
	20	16.39	50.21	-0.0045	0.8088	17.25	4.712	0.9945
	30	24.71	53.44	-0.0052	0.8245	25.33	6.227	0.9922
	40	35.52	54.16	-0.0085	0.7863	36.52	6.335	0.9989
	50	49.61	54.62	-0.0199	0.8421	46.32	6.565	0.9994
DC	10	5.88	44.32	-0.0031	0.7776	6.31	2.001	0.9865
	20	15.91	48.99	-0.0039	0.8548	16.23	4.445	0.9952
	30	23.28	51.27	-0.0048	0.8465	24.15	6.525	0.9991
	40	34.61	53.35	-0.0081	0.8216	35.33	6.561	0.9949
	50	47.21	53.94	-0.0099	0.8333	47.99	6.566	0.9998

Eq. (7) can be rearranged and linearized as,

$$\frac{t}{q_t} = \frac{1}{k_2 q_e^2} + \frac{t}{q_e} \quad (8)$$

The plot t/q_t versus time (t) (Fig. 4) shows the straight line. The second order kinetic values of q_e and k_2 were calculated from the slope and intercept of the plots t/q_t versus t . Table 2 depicts the computed results obtained from first and second order kinetic model for AC and DC source. The calculated q_e values well agree with the experimental q_e values for second order kinetics model better than the first order kinetics model for both AC and DC. These results indicate that the adsorption system belongs to the second order kinetic model.

3.5. Adsorption isotherm

The adsorption capacity of the adsorbent has been tested using Freundlich and Langmuir isotherm and Dubinin–Radushkevich isotherms. To determine the isotherms, the initial pH was kept at 7 and the concentration of cadmium used was in the range of 10–50 mg/L.

3.5.1. Freundlich isotherm

The Freundlich isotherm is an empirical model relates the adsorption intensity of the sorbent towards adsorbent. The isotherm is adopted to describe reversible adsorption and not restricted to monolayer formation. The mathematical expression of the Freundlich model can be written as [37]

$$q_e = KC^n \quad (9)$$

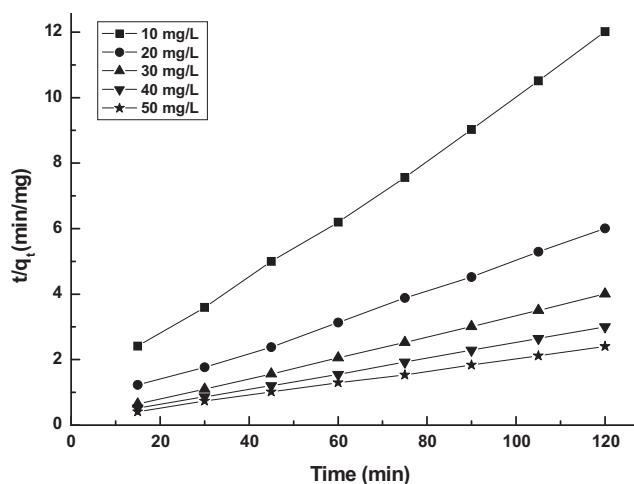


Fig. 4. Second order kinetic model plot of different concentrations of cadmium. Conditions: current density of 0.2 A/dm²; temperature of 303 K; pH of 7.0.

Eq. (9) can be linearized in logarithmic form and the Freundlich constants can be determined as follows [38]

$$\log q_e = \log k_f + n \log C_e \quad (10)$$

where, k_f is the Freundlich constant related to adsorption capacity, n is the energy or intensity of adsorption, C_e is the equilibrium concentration of cadmium. To determine the isotherms, the cadmium concentration used was 10–50 mg/L and at an initial pH 7. The Freundlich constants ' k_f ' and ' n ' values were shown in Table 3 for AC and DC source. It has been reported that values of n lying between 0 and 1 indicate favorable adsorption. From the analysis of the results it is found that the Freundlich plots fit satisfactorily with the experimental data obtained in the present study.

3.5.2. Langmuir isotherm

The Langmuir isotherm is a valid monolayer sorption on a surface containing a finite number of binding sites. It assumes uniform energies of sorption on the surface and no transmigration of sorbate in the plane of the surface.

The linearized form of Langmuir adsorption isotherm model is [39]

$$\frac{C_e}{q_e} = \frac{1}{q_0 b} + \frac{C_e}{q_0} \quad (11)$$

where C_e is the concentration of the cadmium solution (mg/L) at equilibrium, q_0 is the adsorption capacity (Langmuir constant) and b is the energy of adsorption. Fig. 5 shows the Langmuir plot with experimental data. Langmuir plot is a better fit with the experimental data compare to Freundlich plots. The value of the adsorption capacity q_m as found to be 526.33 mg/g and 501.22 mg/g for AC and DC source which is higher than that of other adsorbents studied. The essential characteristics of the Langmuir isotherm can be expressed as the dimensionless constant R_L [40]

$$R_L = \frac{1}{(1 + bC_0)} \quad (12)$$

Table 3

Constant parameters and correlation co-efficient calculated for different adsorption isotherm models at room temperature for cadmium adsorption at 20 mg/L at room temperature.

Isotherm	Constants			
Langmuir	q_m (mg/g)	b (L/mg)	R_L	R^2
	AC	526.33	0.0033	0.8694
DC	501.22	0.0056	0.8661	0.9996
Freundlich	K_f (mg/g)	n (L/mg)	R^2	
	AC	1.348	1.004	0.9841
DC	1.252	1.011	0.9881	
D-R	Q_s ($\times 10^3$ mol/g)	B ($\times 10^3$ mol ² /kJ ²)	E (kJ/mol)	R^2
	AC	0.452	0.2519	7.32
DC	0.488	0.2798	5.22	0.8121

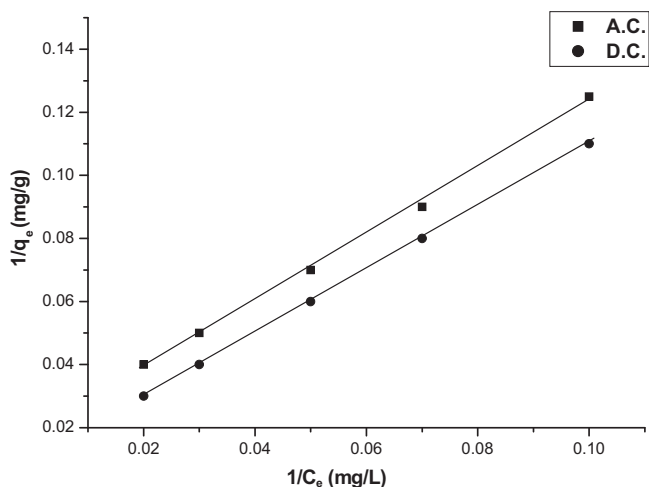


Fig. 5. Langmuir plot ($1/C_e$ versus $1/q_e$). Conditions: pH of 7.0; current density: 0.2 A/dm^2 ; temperature of 303 K; concentration of 10–50 mg/L.

where R_L is the equilibrium constant it indicates the type of adsorption, b , C_0 is the Langmuir constant. The R_L values between 0 and 1 indicate the favorable adsorption.

3.5.3. Dubinin–Radushkevich (D–R) isotherm

Dubinin and Radushkevich have proposed another isotherm which can be used to analyze the equilibrium data. It is not based on the assumption of homogeneous surface or constant adsorption potential, but it is applied to estimate the mean free energy of adsorption (E). This model is given by

$$q_e = q_s \exp(-B\varepsilon^2) \quad (13)$$

where ε is Polanyi potential, equal to $RT \ln(1 + 1/C_e)$, B is related to the free energy of sorption and q_s is the Dubinin–Radushkevich (D–R) isotherm constant [41]. The linearized form is

$$\ln q_e = \ln q_s - 2B RT \ln \left[1 + \frac{1}{C_e} \right] \quad (14)$$

The isotherm constants of q_s and B are obtained from the intercept and slope of the plot of $\ln q_e$ versus ε^2 [42]. The constant B gives the mean free energy of adsorption per molecule of the adsorbate when it is transferred from the solid from infinity in the solution and the relation is given as

$$E = \frac{1}{\sqrt{2B}} \quad (15)$$

The magnitude of E is useful for estimating the type of adsorption process. It was found to be 7.32 and 5.22 kJ/mol for AC and DC, which is smaller than the energy range of adsorption reaction, 8–16 kJ/mol [43]. So the type of adsorption of cadmium on aluminum alloy was defined as chemical adsorption.

The correlation co-efficient values of different isotherm models are listed in Table 3. The Langmuir isotherm model has higher regression co-efficient ($R^2 = 0.999$) when compared to the other models. The adsorption data show good fit to the Langmuir then Freundlich and D–R adsorption isotherm as depicted by the regression coefficient for these systems for both AC and DC. R_L values between 0 and 1.0 further indicate a favorable adsorption of cadmium.

3.6. Effect of temperature

To study the temperature effect, the initial pH was kept at 7 and the concentration of cadmium used was in the range of 10–50 mg/L

Table 4

Pore diffusion coefficients for the adsorption of cadmium at various concentration and temperature.

	Pore diffusion constant $D \times 10^{-9} \text{ (cm}^2/\text{s)}$
Concentration (mg/L)	
10	1.3321
20	0.9541
30	0.9432
40	0.9132
50	0.8945
Temperature (K)	
313	0.7756
323	0.9845
333	1.4456
343	2.0154

for both AC and DC. The amount of cadmium adsorbed on the adsorbent increases by increasing the temperature indicating the process to be endothermic. The diffusion co-efficient (D) for intraparticle transport of cadmium species into the adsorbent particles has been calculated at different temperature by

$$t_{1/2} = \frac{0.03 \times r_0^2}{D} \quad (16)$$

where $t_{1/2}$ is the time of half adsorption (s), r_0 is the radius of the adsorbent particle (cm), D is the diffusion co-efficient in cm^2/s . For all chemisorption system the diffusivity co-efficient should be 10^{-5} – $10^{-13} \text{ cm}^2/\text{s}$ [44]. In the present work, D is found to be in the range of $10^{-9} \text{ cm}^2/\text{s}$. The pore diffusion coefficient (D) values for various temperatures and different initial concentrations of cadmium are presented in Table 4, respectively.

To find out the energy of activation for adsorption of cadmium, the second order rate constant is expressed in Arrhenius form [45].

$$\ln k_2 = \ln k_0 - \frac{E}{RT} \quad (17)$$

where k_0 is the constant of the equation (g/mgmin), E is the energy of activation (J/mol), R is the gas constant (8.314 J/mol K) and T is the temperature in K. Fig. 6 shows that the rate constants vary with temperature according to Eq. (17). The activation energy (0.954 kJ/mol for AC and 0.662 kJ/mol for DC source, respectively) is calculated from slope of the fitted equation. The free energy change is obtained using the following relationship:

$$\Delta G = -RT \ln K_c \quad (18)$$

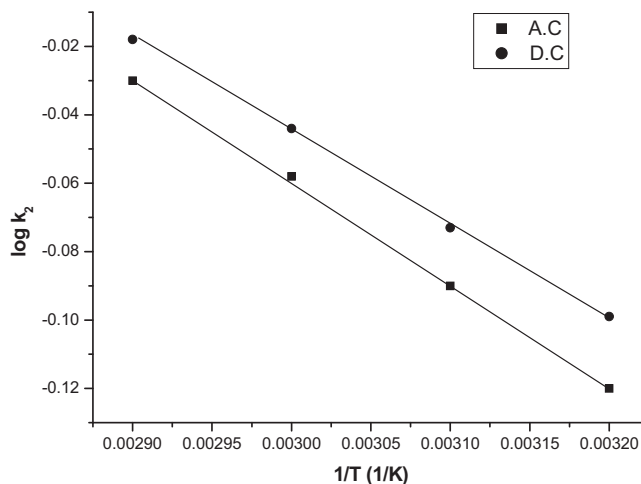


Fig. 6. Plot of $\log k_2$ and $1/T$. Conditions: pH of 7.0; current density of 0.2 A/dm^2 ; temperature of 303 K; concentration of 10–50 mg/L.

Table 5
Thermodynamic parameters for the adsorption of cadmium.

Temperature (K)	AC				DC			
	K_c	ΔG° (J/mol)	ΔH° (kJ/mol)	ΔS° (J/mol K)	K_c	ΔG° (J/mol)	ΔH° (kJ/mol)	ΔS° (J/mol K)
313	1.099	-0.1099			0.9973	-0.0773		
323	1.1142	-0.1154			1.0213	-0.0954		
333	1.1254	-0.3778	6.241	12.638	1.1298	-0.2545	5.663	10.251
343	1.1335	-0.3987			1.1765	-0.3656		

where ΔG is the free energy (kJ/mol), K_c is the equilibrium constant, R is the gas constant and T is the temperature in K. The K_c and ΔG values are presented in Table 5. From the table it is found that the negative value of ΔG indicates the spontaneous nature of adsorption.

Other thermodynamic parameters such as entropy change (ΔS) and enthalpy change (ΔH) were determined using van't Hoff equation,

$$\ln K_c = \frac{\Delta S}{R} - \frac{\Delta H}{RT} \quad (19)$$

The enthalpy change and entropy change were obtained from the slope and intercept of the van't Hoff linear plots of $\ln K_c$ versus $1/T$ (Fig. 7). A positive value of enthalpy change (ΔH) indicates that the adsorption process is endothermic in nature, and the negative value of change in internal energy (ΔG) show the spontaneous adsorption of cadmium on the adsorbent. Positive values of entropy change show the increased randomness of the solution interface during the adsorption of cadmium on the adsorbent. Enhancement of adsorption capacity of electro coagulant (aluminum hydroxide) at higher temperatures may be attributed to the enlargement of pore size and or activation of the adsorbent surface. Using Lagergran rate equation, First order rate constants and correlation co-efficient were calculated for different temperatures (313–343 K). The calculated ' q_e ' values obtained from the first order kinetics agrees with the experimental ' q_e ' values better than the Second order kinetics model. Table 6 depicts the computed results obtained from first and second order kinetic models. These results indicate that the adsorption follows first order kinetic model at different temperatures used in this study.

3.7. Effect of coexisting ions

To study the effect of co-existing ions, in the removal of cadmium, sodium salts of carbonate (0–250 mg/L), phosphate

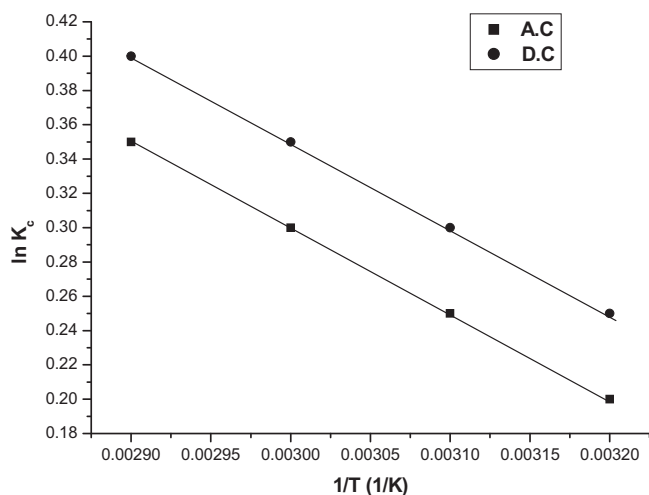


Fig. 7. Plot of $\ln K_c$ and $1/T$. Conditions: pH of 7.0; current density of 0.2 A/dm²; temperature of 303 K; concentration of 10–50 mg/L.

(0–50 mg/L), silicate (0–15 mg/L), and arsenate (0–5.0 mg/L) was added to the electrolyte and electrolysis was carried out using AC with a initial pH of 7 at a temperature of 313 K.

3.7.1. Carbonate

Effect of carbonate (HCO_3^-) on cadmium removal was evaluated by increasing the HCO_3^- concentration from 5 to 250 mg/L in the electrolyte. The removal efficiencies are 97.5, 80, 69.1, 30.2, and 16% for the HCO_3^- ion concentration of 0, 5, 65, 150 and 250 mg/L, respectively. From the results it is found that the removal efficiency of the cadmium is not affected by the presence of HCO_3^- below 5 mg/L. Significant reduction in removal efficiency was observed above 5 mg/L of HCO_3^- concentration is due to the passivation of anode (resulting the hindering of the dissolution process of anode) and the presence of HCO_3^- ion.

3.7.2. Phosphate

The concentration of phosphate (H_2PO_4^- and HPO_4^{2-}) ion was increased from 5 to 50 mg/L, the contaminant range of H_2PO_4^- and HPO_4^{2-} in the ground water. The removal efficiency for cadmium was 97.5, 71.3, 52.6 and 43% for 0, 5, 25 and 50 mg/L of H_2PO_4^- and HPO_4^{2-} ion, respectively. There is no change in removal efficiency of cadmium below 5 mg/L of H_2PO_4^- and HPO_4^{2-} in the water. At higher concentrations (at and above 5 mg/L) of H_2PO_4^- and HPO_4^{2-} , the removal efficiency decreases to 43%. This is due to the preferential adsorption of H_2PO_4^- and HPO_4^{2-} over cadmium as the concentration of H_2PO_4^- and HPO_4^{2-} increase.

3.7.3. Silicate

Effect of silicate on the removal efficiency of cadmium was investigated. The respective efficiencies for 0, 5, 10 and 15 mg/L of silicate are 97.5, 65, 46 and 19%. The removal of cadmium decreased with increasing silicate concentration from 0 to 15 mg/L. In addition to preferential adsorption, silicate can interact with aluminum hydroxide to form soluble and highly dispersed colloids that are not removed by normal filtration.

3.7.4. Arsenate

From the results it is found that the efficiency decreased from 97.5, 81.2, 70.2, 64 to 31% by increasing the concentration of arsenate (H_2AsO_4^- and HAsO_4^{2-}) from 0, 0.5, 1.3 and 5 mg/L. Like phosphate ion, this is due to the preferential adsorption of H_2AsO_4^- and HAsO_4^{2-} over cadmium as the concentration of H_2AsO_4^- and HAsO_4^{2-} increases. So, when H_2AsO_4^- and HAsO_4^{2-} ions present in the water are to be treated which compete greatly with cadmium ions for the binding sites.

3.8. A pilot plant study

A pilot plant capacity cell (Fig. 8) was designed, fabricated and operated for the removal of cadmium from water. The system consists of AC/DC power supply, an electrochemical reactor, a water tank, a feed pump, a flow control valve, a flow measuring unit, a circulation pump, settling tank, sludge collection tank, filtration unit provisions for gas outlet and treated water outlet. The reactor is made of PVC with an active volume of 2000 L. The aluminum

Table 6
Comparison between the experimental and calculated q_e values for different initial cadmium concentrations of 20 mg/L in first and second order adsorption isotherm at various temperatures and pH 7.

Temperature (K)	q_e (exp)	First order adsorption			Second order adsorption		
		q_e (Cal)	K_1 (min/mg)	R^2	q_e (Cal)	K_2 (min/mg)	R^2
313	16.221	15.06	-0.0016	0.7721	16.301	0.1445	0.9954
323	16.323	15.16	-0.0029	0.7752	16.487	0.1654	0.9985
333	16.451	15.76	-0.0036	0.8014	16.556	0.2844	0.9854
343	16.557	15.22	-0.0042	0.7658	16.787	0.3147	0.9957

alloy electrodes (anode and cathode) each consist of five pieces situated approximately 5 mm apart from each other and submerged in the solution. The total electrode surface area is 1500 cm² for both cathodes and anodes. The cell was operated at a current density of 0.2 A/dm² and the electrolyte pH of 7.0. The results showed that the removal efficiency of 97.5 and 96.2% with the energy consumption of 0.454 and 1.002 kWh kl⁻¹ was achieved at a current density of 0.2 A/dm² and pH of 7.0 using aluminum alloy as electrodes using AC and DC, respectively. The results were consistent with the results obtained from the laboratory scale, showing that the process was technologically feasible.

3.9. Surface characterization

3.9.1. SEM and EDAX characterization

In order to gain more insight into the effect of alternating current, the morphology of the electrode surface after two kinds of electrolysis (AC and DC) was characterized by SEM as shown in Fig. 9(a) and (b). It can be observed that when the AC was fed, less disordered pores formed and a smooth microstructure of aluminum suggesting the aluminum electrodes were dissolved uniformly during the electrolysis. While for the electrodes fed with DC, the electrode surface is found to be rough, with a number of dents. These dents are formed around the nucleus of the active sites where the electrode dissolution results in the production of aluminum hydroxides. The formation of a large number of dents may be attributed to the anode material consumption at active sites due to the generation of oxygen at its surface.

Energy-dispersive analysis of X-rays was used to analyze the elemental constituents of cadmium-adsorbed aluminum hydroxide (Fig. 10). It shows that the presence of cadmium, Al and O appears in the spectrum. EDAX analysis provides direct evidence that cadmium is adsorbed on aluminum hydroxide.

3.9.2. XRD studies

X-ray diffraction spectrum of aluminum electrode coagulant showed very broad and shallow diffraction peaks (Fig. 11). This broad humps and low intensity indicate that the coagulant is amorphous

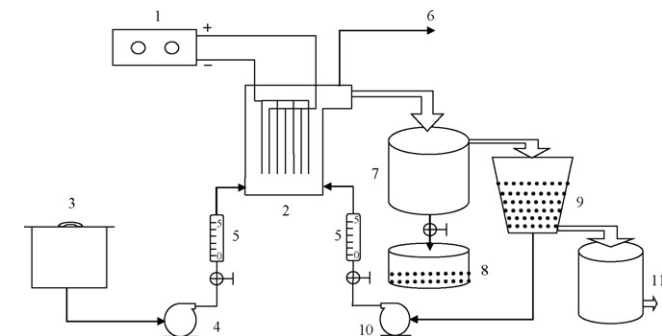


Fig. 8. Flow diagram of the pilot plant electrocoagulation system. 1. AC/DC power supply, 2. electro coagulation cell, 3. water tank, 4. inlet pump, 5. flow meter, 6. gas outlet, 7. setting tank, 8. sludge collection tank, 9. filtration unit, 10. recirculation pump and 11. treated water.

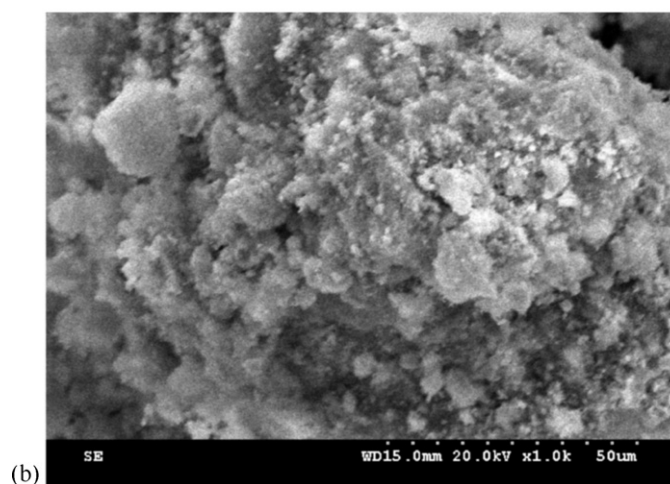
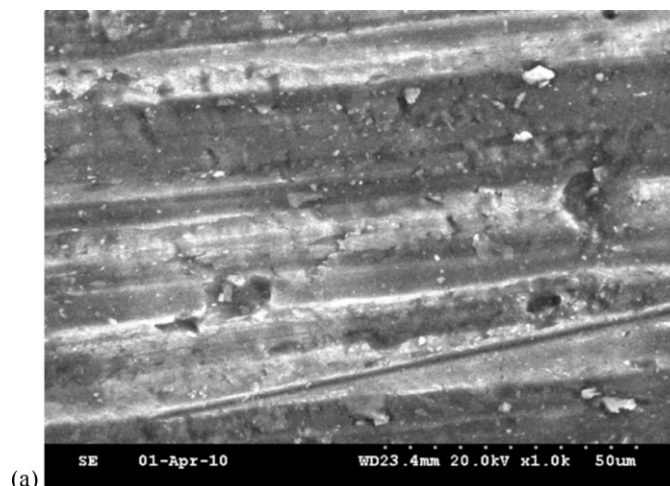


Fig. 9. SEM images of the anode after electrocoagulation by (a) AC and (b) DC.

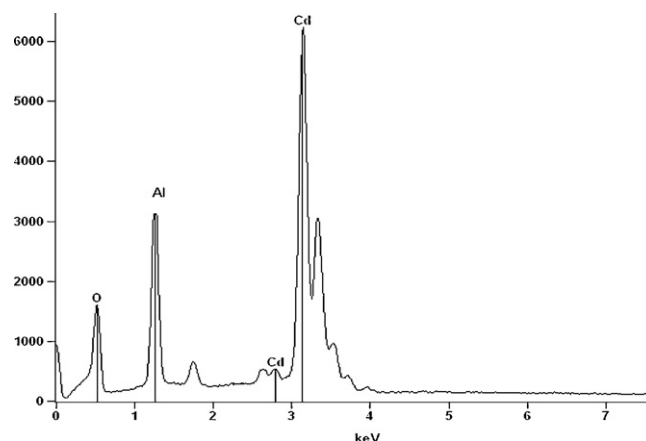


Fig. 10. EDAX spectrum of cadmium-adsorbed aluminum hydroxide.

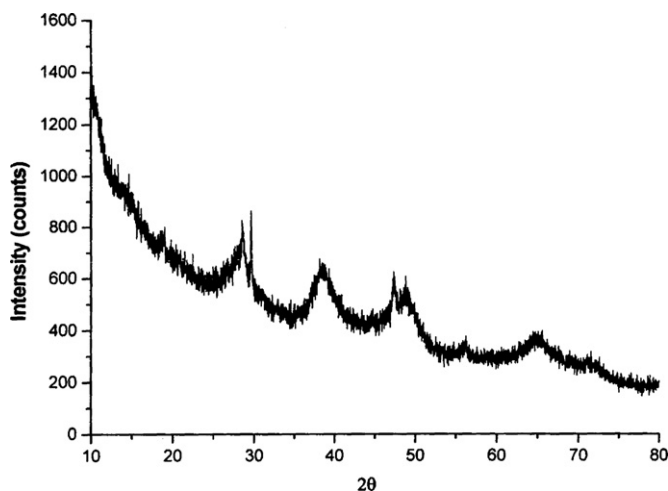


Fig. 11. FTIR spectrum of cadmium-adsorbed aluminum hydroxide.

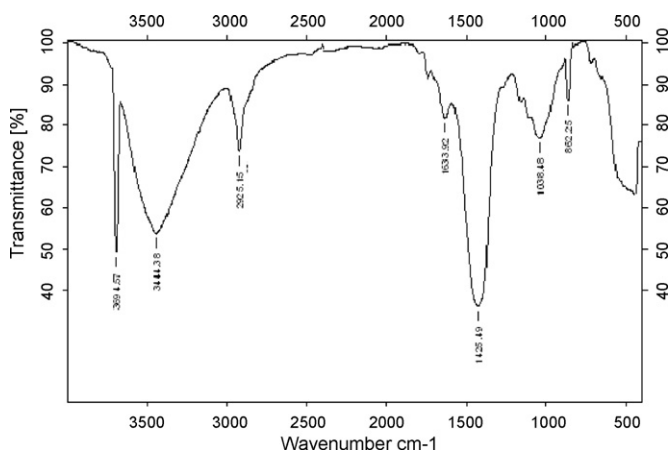


Fig. 12. FTIR spectrum of cadmium-adsorbed aluminum hydroxide.

or very poor crystalline in nature. It is reported [46] that the crystallization of aluminum hydroxide is a very slow process resulting all aluminum hydroxides found to be either amorphous or very poorly crystalline. The literature on the amorphous nature of aluminum oxide layer supported the present results [46].

3.9.3. FTIR studies

Fig. 12 presents the FT-IR spectrum of cadmium–aluminum hydroxide. The sharp and strong peak at 3444.38 cm^{-1} is due to the O–H stretching vibration in the $\text{Al}(\text{OH})_3$ structures. The 1633.92 cm^{-1} peak indicates the bent vibration of H–O–H. The strong peak at 1038.48 cm^{-1} is assigned to the Al–O–H bending. Cd–O vibration at 862.25 cm^{-1} also observed.

4. Conclusion

The results showed that the optimized removal efficiency of 97.5% and 96.2% was achieved for AC and DC source at a current density of 0.2 A/dm^2 and pH of 7.0 using aluminum alloy as anode and cathode. The aluminum hydroxide generated in the cell remove the cadmium present in the water and to reduce the cadmium concentration to less than 0.005 mg/L , and made it for drinking. The results indicate that the process can be scaled up to higher capacity. For both AC and DC electrolysis the adsorption of cadmium preferably fitting Langmuir adsorption isotherm better than Freundlich isotherm. The adsorption process follows second order kinetics. Temperature studies showed that adsorption was endothermic and

spontaneous in nature. From the surface characterization studies, it is confirmed that the aluminum hydroxide generated in the cell adsorbed cadmium present in the water.

Acknowledgment

The authors wish to express their gratitude to the Director, Central Electrochemical Research Institute, Karaikudi to publish this paper.

References

- [1] O.J. Nrlagu, M.J. Pacyna, Quantitative assessment of worldwide contamination of air, water and soils by trace metals, *Nature* 333 (1988) 134–139.
- [2] M. Tsezos, Biosorption of metals. The experience accumulated and the outlook for technology development, *Hydrometallurgy* 59 (2001) 241–243.
- [3] K. Bedow, I. Bekri-Abbes, E. Srasra, Removal of cadmium (II) from aqueous solution using pure Smectite and Lewatite S 100: the effect of time and metal concentration, *Desalination* 223 (2008) 269–273.
- [4] K. Nogawa, E. Kobayashi, Y. Okubo, Y. Suwazono, Environmental cadmium exposure, adverse effects and preventive measures in Japan, *Biometals* 17 (2008) 581–587.
- [5] H.A. Schroede, Cadmium as a factor in hypertension, *J. Chronic Dis.* 18 (1965) 647–656.
- [6] T.H. Bui, J. Lindsten, G.F. Nordberg, Chromosome analysis of lymphocytes from cadmium workers and itai-itai Patients, *Environ. Res.* 9 (1975) 187–195.
- [7] IARC, Beryllium, Cadmium, Mercury and Exposures in the Glass Manufacturing Industry Monographs on the Evaluation of Carcinogenic Risks to Humans, vol. 58, 1994, pp. 444–447.
- [8] Central Pollution Control Board, Ministry of Environment and Forests, Govt. of India, Delhi. <http://www.cpcb.nic.in>.
- [9] D.G. Kinniburgh, M.L. Jackson, in: M.A. Anderson, A.J. Rubin (Eds.), *Adsorption of Organics at Solid–Liquid Interfaces*, Ann Arbor Science Publishers, Ann Arbor, MI, 1981, p. 91.
- [10] M.S. Rahman, M.R. Islam, Adsorption of Cd(II) ions from synthetic waste water using maple sawdust, *Energy Sources, Part A* 32 (2010) 222–231.
- [11] S.C. Ibrahim, M.A.K. Hanafiah, M.Z.A. Yahya, Removal of cadmium from aqueous solutions by adsorption onto sugarcane, *Am. Eurasian J. Agric. Environ. Sci.* 3 (2006) 179–187.
- [12] M.A.K. Megat Hanafiah, M.Z.A. Yahya, H. Zakaria, S.C. Ibrahim, Adsorption of Cd(II) ions from aqueous solutions by *Lang (Imperata cylindrica)* leaf powder: effect of physiochemical environment, *J. Appl. Sci.* 7 (2007) 489.
- [13] A. Archana, K.K. Sahu, Kinetic and isotherm studies of cadmium adsorption on manganese nodule residue, *J. Hazard. Mater.* 137 (2007) 915.
- [14] E.J. Chou, Y. Okamoto, Removal of cadmium ion from aqueous solutions, *J. Water. Pollut. Control Fed.* 48 (1976) 2747–2753.
- [15] J.K. Salpathy, M. Chaudhuri, Treatment of cadmium-plating and chromium-plating wastes by iron-coated sand, *Water Environ. Res.* 6 (7) (1995) 788–790.
- [16] C.A. Cristofoli, L. Axe, Competition of Cd, Cu, and Pb Adsorption on Goethite, *J. Environ. Eng.* 126 (2000) 67.
- [17] J.L. Gardea-Torresdey, G. de la Rosa, J.R. Peralta-Videa, Use of phytofiltration technologies in the removal of heavy metals: a review, *Pure Appl. Chem.* 76 (2004) 801–813.
- [18] M. Ajmal, R.A. Rao, S. Anwar, J. Ahmad, R. Ahmad, Adsorption studies on rice husk: removal and recovery of Cd (II) from wastewater, *Bioresour. Technol.* 86 (2003) 147–149.
- [19] W.S. Peternele, A.A. Winkler-Hechenleitner, E.A. GomezPineda, Adsorption of Cd (II) and Pb (II) on to functionalized formic lignin from sugar cane bagasse, *Bioresour. Technol.* 6 (8) (1999) 95–100.
- [20] A. Saeed, M. Iqbal, Bioremoval of cadmium from aqueous solution by gram husk, *Water Res.* 3 (7) (2003) 3472–3484.
- [21] D.P. Tiwari, D.K. Singh, D.N. Saksena, Removal of cadmium from wastewater, *J. Environ. Eng.* 121 (1995) 479–484.
- [22] W.E. Marshall, M. Johns, Agricultural by-products as metal adsorbents: sorption properties and resistance to mechanical abrasion, *J. Chem. Technol. Biotechnol.* 66 (1996) 192–198.
- [23] I.B. Abbes, S. Bayoudh, M. Baklouti, Converting waste polystyrene into adsorbent: potential use in the removal of lead and cadmium ions from aqueous solution, *J. Polym. Environ.* 14 (2006) 249–256.
- [24] S.I. Haider Taqvi, S.M. Hasany, M. Iqbal Bhangar, Sorption profile of Cd(II) ions onto beach sand from aqueous solutions, *J. Hazard. Mater.* 141 (2007) 37–44.
- [25] S. Kocaoba, G. Akcin, Removal of chromium (III) and cadmium (II) from aqueous solutions, *Desalination* 180 (2005) 151–156.
- [26] S. Vasudevan, J. Lakshmi, J. Jayaraj, G. Sozhan, Remediation of phosphate – contaminated water by electrocoagulation with aluminium, aluminium alloy and mild steel anodes, *J. Hazard. Mater.* 164 (2009) 1480–1486.
- [27] X. Chen, G. Chen, P.L. Yue, Investigation on the electrolysis voltage of electrocoagulation, *Chem. Eng. Sci.* 5 (7) (2002) 2449–2455.
- [28] J.Q. Jiang, N. Graham, C. André, G.H. Kelsall, N. Brandon, Laboratory study of electro-coagulation–flotation for water treatment, *Water Res.* 3 (6) (2002) 4064–4078.

- [29] S. Vasudevan, S. Margrat Sheela, J. Lakshmi, G. Sozhan, Optimization of the process parameters for the removal of boron from drinking water by electrocoagulation – a clean technology, *J. Chem. Technol. Biotechnol.* 85 (2010) 926–933.
- [30] S. Vasudevan, G. Sozhan, S. Ravichandran, J. Jayaraj, J. Lakshmi, S. Margrat Sheela, Studies on the removal of phosphate from drinking water by electrocoagulation process, *Ind. Eng. Chem. Res.* 4 (7) (2008) 2018–2023.
- [31] G. Chen, Electrochemical technologies in wastewater treatment, *Sep. Purif. Technol.* 3 (8) (2004) 11–41.
- [32] C. Namasivayam, A. Ranganathan, Removal of Cd (II) from wastewater by adsorption on waste Fe(III)/Cr(III) hydroxide, *Water Res.* 29 (1995) 1737–1744.
- [33] K. Nadhem Hamadi, M. Xiao Dong Chen, G.Q. Mohammed Farid, L. Max, Adsorption kinetics for the removal of chromium(VI) from aqueous solution by adsorbents derived from used tyres and sawdust, *Chem. Eng. J.* 84 (2001) 95–105.
- [34] M.S. Gasser, G.H.A. Morad, H.F. Aly, Batch kinetics and thermodynamics of chromium ions removal from waste solutions using synthetic adsorbents, *J. Hazard. Mater.* 142 (2007) 118–129.
- [35] F.H. Uber, Die Adsorption in Losungen, *Z. Phys. Chem.* 57 (1985) 387–389.
- [36] C. Namasivayam, K. Prathap, Recycling Fe(III)/Cr(III) hydroxide, an industrial solid waste for the removal of phosphate from water, *J. Hazard. Mater.* 123B (2005) 127–135.
- [37] I. Langmuir, The adsorption of gases on plane surfaces of glass, mica and platinum, *Am. Chem. Soc.* 40 (1918) 1361–1403.
- [38] L. Michelson, P.G. Gideon, E.G. Pace, L.H. Kutal, Office Water Res. Technol. Bull. 265 (1965).
- [39] H. Demiral, I. Demiral, F. Tumsek, B. Karacacakoglu, Adsorption of chromium(VI) from aqueous solution by activated carbon derived from olive bagasse and applicability of different adsorption models, *Chem. Eng. J.* 14 (4) (2008) 184–188.
- [40] E. Oguz, Adsorption characteristics and the kinetics of the Cr(VI) on the *Thuja orientalis*, *Colloids Surf.* 25 (2) (2005) 121–128.
- [41] I.A.W. Tan, B.H. Hameed, A.L. Ahmed, Equilibrium and kinetic studies on basic dye adsorption by oil palm fibre activated carbon, *Chem. Eng. J.* 12 (7) (2007) 111–119.
- [42] X.Y. Yang, B. Al-Duri, Application of branched pore diffusion model in the adsorption of reactive dyes on activated carbon, *Chem. Eng. J.* 83 (2001) 15–23.
- [43] A.K. Golder, A.N. Samantha, S. Ray, Removal of phosphate from aqueous solution using calcined metal hydroxides sludge waste generated from electrocoagulation, *Sep. Purif. Technol.* 5 (2) (2006) 102–108.
- [44] M. Yurdakoc, Y. Seki, S. Karahan, K. Yurdakoc, Kinetic and thermodynamic studies of boron removal by Siral 5, Siral 40, and Siral 80, *J. Colloid Interface Sci.* 286 (2005) 440–446.
- [45] S. Vasudevan, J. Lakshmi, G. Sozhan, Studies on the removal of iron from drinking water by electrocoagulation – a clean process, *Clean* 37 (2009) 45–51.
- [46] A.J.G. Gomes, P. Daida, M. Kesmez, M. Wei, H. Moreno, R.J. Parga, G. Irwin, H. McWhinney, T. Grady, E. Peterson, L.D. Cocke, Arsenic removal by electrocoagulation using combined Al–Fe electrode system and characterization of products, *J. Hazard. Mater. B* 139 (2007) 220–227.